ISSN (Print) 1226-1750
ISSN (Online) 2233-6656
Journal of Magnetics 23(2), 142-151 (2018) https://doi.org/10.4283/JMAG.2018.23.2.142

Study on Detection Methods of Residual Wall Thickness for Process Pipeline Corrosion in Oil and Gas Gathering and Transportation Station

Mingjiang Shi*, Honghui Zhao, Zhiqiang Huang, and Lu Jiang

School of Mechanical Engineering, Southwest Petroleum University, Chengdu 610500, China

(Received 2 February 2018, Received in final form 13 May 2018, Accepted 17 May 2018)

In this paper, it is proposed to adopt Pulsed Eddy Current (PEC) testing of coaxial double coil structure to implement the detection on residual wall thickness of pipeline corrosion in oil and gas gathering and transportation station, in the view of reduction of wall thickness caused by corrosion. The electromagnetic field theory is applied to conduct theoretical analysis on PEC detection. On such basis, a theoretical model of coaxial double coil structure for PEC detection is built, and the relation of voltage phase of the detected signal varying with the wall thickness of the pipeline is derived. Then a method for evaluating the residual wall thickness of pipelines based on the phase trough time of PEC signals is proposed. Moreover, the parameters of the PEC probe are optimized by finite element method, and the detection system is designed accordingly. As a result, the practicability of the detection system and the correctness of the theoretical model are verified by experiments, proved that the model can realize the detection of the residua wall thickness under the condition of different media transported by the pipeline.

Keywords : pipeline, thickness, PEC, optimal design

1. Introduction

Oil-gas gathering and transportation station, as the important hinge in the whole petroleum extraction & production system, undertakes the tasks of collection, storage, processing, handling, and transportation of crude oil and natural gas. It is normally characterized by complicated piping layout, relatively big pipe diameter, small transportation pipeline, and changeable media (including water, oil, gas and various mixed media) passing through the pipeline. Compared with long transportation pipeline, it is more vulnerable to internal corrosion damage due to the diversity of medium in process piping [1, 2]. In addition, under the combined effects of inner defects of pipeline and changes of environment, the process piping will be damaged and corroded in various degrees, which has become an important factor threatening the safety of oil and gas gathering & transportation station.

The eddy current testing technique is important method of the industrial non-destructive test. Since there is no coupling agent, no closely contact of tested materials or work pieces, the nature of the tested materials or the work pieces will not be influenced in the process of test. For these merits, this technique is widely used. Currently, the eddy current testing technique main includes remote field eddy current testing, multi-frequency eddy current testing and pulsed eddy current (pulsed eddy current, PEC) [3]. Remote field eddy current detection applies remote field eddy current effect is to keep a two to three times diameter of the pipe between excitation coil and tested coil to gain a detection capability penetrating pipe wall. Generally, it detects inside the pipeline in the form of internal communication to transform excitation frequency into low frequency communication.

The disadvantage of remote field eddy current detection is that the overall length of the probe is too large, and the distance between the excitation coil and the detecting coil is even larger, resulting in extremely low signal amplitude, which means high-power excitation source should be adopted. Furthermore, the low frequency communication excitation also limits the scanning speed of the detection [4, 5]. Multi-frequency eddy current testing adopts two or more excitation probes with different frequencies for detection based on traditional single frequency eddy current technique. For this detection technique, each probe is processed separately, and the data of multiple probes are

*Corresponding author: Tel: +86-028-8303-7203
Fax: +86-028-8303-7209, e-mail: swpushi@126.com

finally integrated. This technique with the advantage of the adoption of excitation probe with multiple frequencies can effectively reduce the impact of external interference on a single frequency. However, the disadvantage is that it is required to add probes for better results. As a result, the size of instrument should be enlarged, and the detection information obtained is also limited [6].

As known, PEC detection technique is a new branch of eddy current detection technology [7, 8]. The pulse signal is synthesized by sinusoidal signals of different frequencies. Namely the pulse signal contains a wider spectrum. Compared with a single frequency excitation signal, the signal detected by the pulse excitation contains more information about the specimen [9-11]. If the pulse excitation frequency remains unchanged, only one scanning will be needed to complete the extraction of multiple information in the specimen [12]. Meanwhile, it has the characteristics of electromagnetic non-contact coupling. The time-domain transient analysis is carried out in the induced magnetic field by the pulsed eddy current and the time of the peak in the induced magnetic field from the test is directly used for the flaw detection. The signals of pulse eddy current response quicker than the ones of multi-frequency current.

Considering the complicated environment of the oil pipeline and other substances, e.g. wax, attached in the oil pipe wall in oil gathering & transportation station, a PEC testing method based on coaxial double coil structure is proposed in this paper. The voltage model of PEC testing is established, and the finite element software COMSOL is used to establish the detection simulation model and optimize the probe parameters. The eddy current testing model is analyzed theoretically from circuit, and the relationship between the voltage phase of detection signal varying from different wall thickness is gained. Moreover, an evaluation method to residual wall thickness based on phase trough time of induction voltage is also proposed, and the effectiveness of the proposed method is verified by the signals measured from PEC test to residual wall thickness of pipeline corrosion.

2. Coil Induced Voltage Model

2.1. Detection principle of PEC

The detection principle of PEC is as shown in Fig. 1:

If the excitation coil is imposed with a periodic square wave excitation signal with certain duty cycle, an alternating source magnetic field will be generated around the excitation coil to cause a rapidly decaying PEC generated in detected pipe wall. The pulsed eddy will produce an alternating reflected magnetic field around itself. Under the combined effects of the reflected magnetic field and the source magnetic field, a transient induced voltage varying with PEC will be generated in detection coil. If the wall thickness of the tested pipeline changes, the distribution of the induced eddy will be affected, which will affect the reflected magnetic field, and finally change the transient induced voltage on the detection coil. Therefore, the thickness of the pipeline can be quantitatively analyzed by detecting and observing the changes of the transient induced voltage signal.

2.2. Coaxial double coil model

In order to achieve an effective detection, when using the approach as shown in Fig. 2, the time domain signal of induction voltage can be enabled to the highest level, as well as the detection sensitivity on wall thickness of ferromagnetic pipe [13].

2.3. Equivalent circuit on PEC detection

In actual detection, the excitation coil and the detection

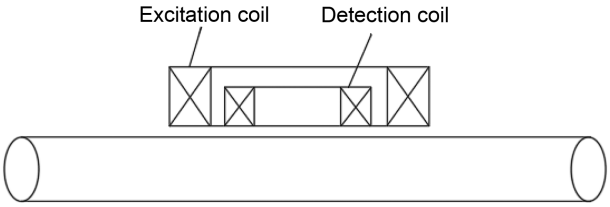

Fig. 2. Relative location diagram of coil oil pipe.

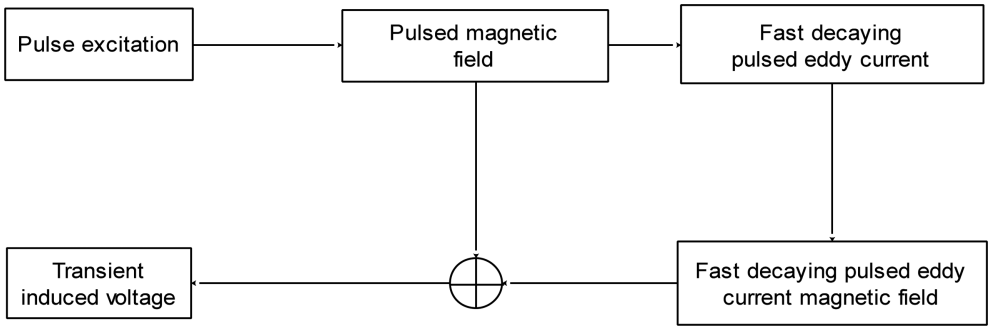

Fig. 1. PEC detection principle.

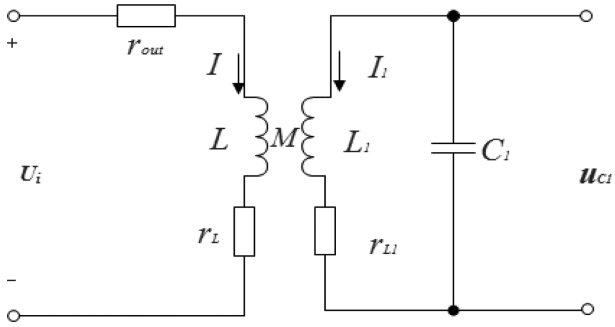

Fig. 3. Pulse current detection equivalent circuit.

coil are made close to pipeline detected to form coupling circuit, the common reactance of the primary coil L and the secondary coil L_1 is represented by M. The equivalent circuit of PEC testing is made shown in Fig. 3.

Where, U_i is excitation voltage, r_{out} is excitation power output impedance, r_L is the self-resistance of primary coil L, r_{L1} is the self-resistance of secondary coil L_1, and C_1 is the distributed capacitance in measuring loop.

2.4. Induced voltage deduction

As shown in Fig. 3, for the PEC test equivalent circuit, under the action of jump function 0-U_0 voltage, it can be obtained:

$$U_i - M\frac{\mathrm{d}I_1}{\mathrm{d}t} = IR + L\frac{\mathrm{d}I}{\mathrm{d}t} \tag{1}$$

$$-M\frac{\mathrm{d}I}{\mathrm{d}t} = R_1 I_1 + L_1\frac{\mathrm{d}I_1}{\mathrm{d}t} + \frac{Q}{C_1} \tag{2}$$

$$M = K\sqrt{LL_1} \tag{3}$$

$$R = r_{out} + r_L \tag{4}$$

$$R_1 = r_{L1} \tag{5}$$

Where, M is the common reactance of the primary coil L and the secondary coil L_1, K is coupling coefficient, excitation power output impedance r_{out} and the self-resistance r_L of coil L are included in the primary loop resistance R, while only the self-residence r_{L1} of secondary coil L_1 is included in secondary loop resistance R_1, by derivation on both sides of formula 2, it is concluded:

$$-M\frac{\mathrm{d}^2 I}{\mathrm{d}t^2} = R_1\frac{\mathrm{d}I_1}{\mathrm{d}t} + L_1\frac{\mathrm{d}^2 I_1}{\mathrm{d}t^2} + \frac{I_1}{C_1} \tag{6}$$

Combined with circuit transition process theory, we can assume that $I = A[1 - \exp(-\alpha t)]$, then the current I shall be: when $t = \infty$, $I = \frac{U_i}{R}$. Thus it is determined $A = \frac{U_i}{R}$. Therefore, I can be expressed as:

$$I = \frac{U_i}{R}[1 - \exp(-\alpha t)] \tag{7}$$

Supposing $I_1 = B\exp(-\alpha t)$, where B is arbitrary constant, I and I_1 can be substituted to formula 1 to gain:

$$U_i + MB\alpha\exp(-\alpha t) = U_i[1 - \exp(-\alpha t)] + L\frac{U_i}{R}\alpha\exp(-\alpha t) \tag{8}$$

$$\Rightarrow \alpha = \frac{U_i}{\frac{L}{R}U_i - MB} \tag{9}$$

Then I and I_1 are substituted to formula 6:

$$M\frac{U_i}{R}\alpha^2 = -R_1 B\alpha + L_1 B\alpha^2 + \frac{1}{C_1}B \tag{10}$$

$$\Rightarrow B = \frac{M\frac{U_i}{R}\alpha^2}{L_1\alpha^2 - R_1\alpha + \frac{1}{C_1}} \tag{11}$$

The value of the distributed capacitance C_1 in the secondary (detection) loop is very small, for Nano farad level. Therefore, the value of $\frac{1}{C_1}$ is extreme large, and the other two items in the upper denominator can be ignored, thus:

$$B = C_1 M\frac{U_i}{R}\alpha^2 \tag{12}$$

After substituting the above formula to formula 9, it can be gained:

$$\alpha = \frac{U_i}{\frac{L}{R}U_i - C_1 M^2\frac{U_i}{R}\alpha^2} \tag{13}$$

As the value of C_1 is small, therefore, the item behind the upper denominator can be ignored, then:

$$\alpha = \frac{R}{L} \tag{14}$$

After substituting α to formula 11, it can be gained:

$$B = C_1 M\frac{U_i}{R}\frac{R^2}{L^2} = C_1 U_i\frac{M}{L}\frac{R}{L} \tag{15}$$

After substituting α and B into I_1, the current in secondary circuit is:

$$I_1 = C_1 U_i\frac{MR}{L}\exp\left(-\frac{R}{L}t\right) \tag{16}$$

That is, the voltage of distributed capacitor C_1 of secondary circuit?

$$u_{C_1} = \frac{1}{C_1}\int_0^t I_1 \mathrm{d}t = \frac{M}{L}U_i\left[1 - \exp\left(-\frac{R}{L}t\right)\right] \quad (17)$$

Figure 3 shows the equivalent circuit of pulsed eddy current, as shown, inductance, capacitance and resistance exist in the circuit, and with the change of the thickness of the pipe wall, the impedance in the circuit is affected. It can be judged from formula 17 that the voltage signal in the detecting coil is exponentially attenuated by the influence of the thickness of the pipe wall, as the peak value of the induced voltage varies non-linearly with the wall thickness [14]. In practice, it is difficult to calibrate. Therefore, the Hilbert transform is used to derive the relation of the phase information of the voltage signal, varying with the wall thickness in the detection coil.

The expressions of the Hilbert transform in time domain can be expressed by the following formula [15-17]:

$$y(t) = x(t)\frac{1}{\pi t} \quad (18)$$

That is, the Hilbert transformation of function $x(t)$ is the convolution of the convolution function and $1/(\pi t)$ [18].

The Fourier transformation of $1/(\pi t)$ is:

$$F\left(\frac{1}{\pi t}\right) = -j\,\mathrm{sign}(f) \quad (19)$$

Therefore, the Fourier transformation of $x(t)$ is:

$$\hat{x}(f) = (f) - j\,\mathrm{sign}(f) \quad (20)$$

As shown from the above formula, the Fourier transformation of $x(t)$ is to make phase shift of signal $x(t)$ in frequency domain, when $f > 0$, $x(t)$ shifts $-\pi/2$ in the frequency domain, when $f < 0$, $x(t)$ shifts $\pi/2$ in frequency domain. Therefore, the gained Fourier transformation of $x(t)$ can firstly make FFT transformation to $x(t)$, and then the phase shifts. Finally, it is gained by FFT transformation. The results of Hilbert transformation conducted by the above steps to the voltage of distributed capacitor C_1 of secondary circuit, that is, formula 17 are:

$$\hat{u}_{C_1} = \frac{M}{L}U_i\left[1 - \exp\left(-\frac{R}{L}t\right)\right]\exp\left(\frac{2\pi MU_i}{L}\left(1 - \exp\left(\frac{R}{L}t\right)\right)\right) \quad (21)$$

Then, the analytic signal of $\hat{u}_{C_1}$ is

$$U_{c_1} = u_{C_1} + j\hat{u}_{C_1} \quad (22)$$

Instantaneous phase of u_{C_1} is :

$$\theta = \arctan\frac{\hat{u}_{C_1}}{u_{C_1}} = \arctan\left(\exp\left(\frac{2\pi tMU_i}{L}\left(1 - \exp\left(\frac{R}{L}t\right)\right)\right)\right) \quad (23)$$

R/L will be large when the wall thickness of the pipe becomes thin, as known from formula 23. If the phase size of the tube reaches no change with the wall thickness, the time required increases. In addition, when the inductor L is charged, the current I approaches the saturation value, and the change rate $\frac{\mathrm{d}I}{\mathrm{d}t}$ will be smaller and smaller, and voltage $-M\frac{\mathrm{d}I}{\mathrm{d}t}$ generated in secondary circuit will approach to 0.

3. Finite Element Model of Process Pipeline Residual Wall Thickness in the Station

3.1. Finite element model of pipeline residual wall thickness detection

The eddy current density produced by alternating incident magnetic field in the tube wall decays exponentially from top to bottom, and it is densest in the surface portion of the pipe, when the attenuation to the surface density of $1/e$ is 37 % [19]. The eddy penetration depth is called standard penetration depth. Its calculation formula is as shown in formula 24, where, δ is standard penetration depth (m); σ is electrical conductivity (S/m) of materials; μ is the permeability of materials; and ω is the angular frequency (rad/s).

$$\delta = \sqrt{\frac{2}{\omega\sigma\mu}} \quad (24)$$

The expression of penetration depth as shown in the formula 24 only applies to the single frequency current. As for the pulsed current, the formula cannot be used directly. According to formula spread by the Fourier series, one pulsed signal can spread to the combinations which include fundamental wave and many harmonic components. If a square wave is defined with the period of T, the width of the pulse of Δ, the pulse waveform as shown in Fig. 4. Then the expanded form of the Fourier series is:

$$g(t) = A_0 + \sum_{n=1}^{\infty} A_n \sin(n\omega_1 t + \phi) \quad (25)$$

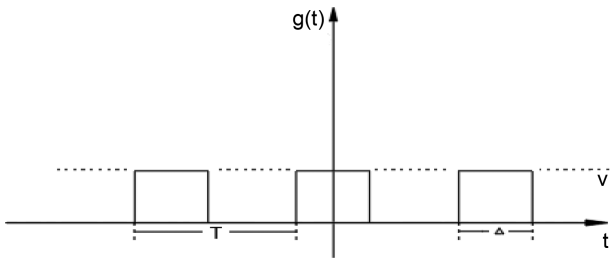

Fig. 4. Typical excitation pulse signal diagram.

Where, ω_1 is frequency of the reference angle, A_n is amplitude spectrum, and ϕ is phase spectrum.

From the above, the frequency of the reference angle and the amplitude spectrum are:

$$\omega_1 = 2\pi f_1 \tag{26}$$

$$A_n = \frac{2V}{n\pi}\left|\sin\left(\frac{n\pi\Delta}{T}\right)\right| \tag{27}$$

The chosen pulse width and period should satisfy the pulse signals of $T = 2\Delta$, then the frequency of the reference angle is expressed as:

$$\omega_1 = 2\pi f = 2\pi\frac{1}{T} = \frac{\pi}{\Delta} \tag{28}$$

Then the weight of all the frequency of excitation pulse signals ω is:

$$\omega = n\omega_1 = n\frac{\pi}{\Delta},\ n = 1, 3, 5,. 7, ..., \infty \tag{29}$$

After substituting formula 29 to formula 24, it can be gained:

$$\delta = \sqrt{\frac{2\Delta}{n\pi\sigma\mu}},\ n = 1, 3, 5, 7, ..., \infty \tag{30}$$

When $n = 1$, which means the frequency of the reference angle is used, the standard depth of penetration δ_w of the gained pulse current is as follows:

$$\delta_w = \sqrt{\frac{2\Delta}{\pi\sigma\mu}} \tag{31}$$

Where, δ_w is the skin depth of pulse current (m), Δ is pulse width(s), σ is conductivity (S/m), and μ is permeability (H/m).

As shown in formula 31 that to add the pulse width and period can increase the penetration depth of the pulse current, which means to decrease the pulse excitation frequency and increase the duty ratio of the pulse. That is good for testing the in-depth flaws in order to avoid the missing inspections. The article chooses the signals of 50 % duty ratio and change the width of the pulse via controlling the excitation frequency of pulse. In this way, it can reach the detection requirement.

When the thickness of the specimen is greater than the depth of penetration, the thickness has almost no influence on the coil impedance. In order to study the distribution of eddy current in the pipe to ensure that the thickness of the pipe is less than the depth of penetration, the finite element model of pipeline residual wall thickness detection is established using COMSOL as shown in Fig. 5. The object is a well lined 6mm thickness pipe.

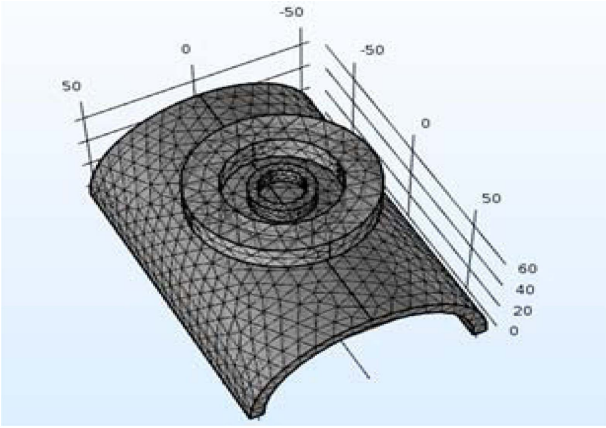

Fig. 5. (Color online) Finite element model of pipeline residual wall thickness detection.

3.2. Model parameter optimization

3.2.1. Influence of excitation frequency on detection signal

The signal used in PEC testing is square wave exciting signal, while the frequency signals contained in the pulse signal range are widely from low frequency to high frequency. As affected by conductor skin effect, the penetration depth of eddy current in the specimen is affected by frequency, as known from formula 24. The penetrability of PEC generated by low-frequency excitation signal is strong; the detection signal is strong and the sensitivity is high; and the detection and resolution on wall thickness are better. However, the penetration of the PEC generated by the high-frequency signal is relatively weaker. Its effect of wall thickness detection is relatively poor, especially when the detection depth is larger, and the effect is less obvious. 4 Hz, 10 Hz, 20 Hz, 40 Hz and 50 Hz are used as excitation signal frequency respectively for detection on pipes with a thickness of 6mm. The results are as shown in Fig. 6.

As shown, the magnitude of the induced voltage varies accordingly as the frequency changes. The maximum amplitude is found at 10 Hz. The larger the frequency, the smaller the value is after 10 Hz, and after 40 Hz. The attenuation of the signal has become distorted, as a result, the effect of greater frequency is not continued to observe. In addition, the conductor skin effect of formula 24 shows that the greater the frequency, the smaller the penetration depth of the eddy will be. Therefore, in order to obtain large penetration depth and obtain good detection signals, the excitation frequency is chosen as 10 Hz.

3.2.2. Influence of coil turns on detection signal

3.2.2.1. Number of turns of excitation coil

With constant excitation voltage, the impedance of coil

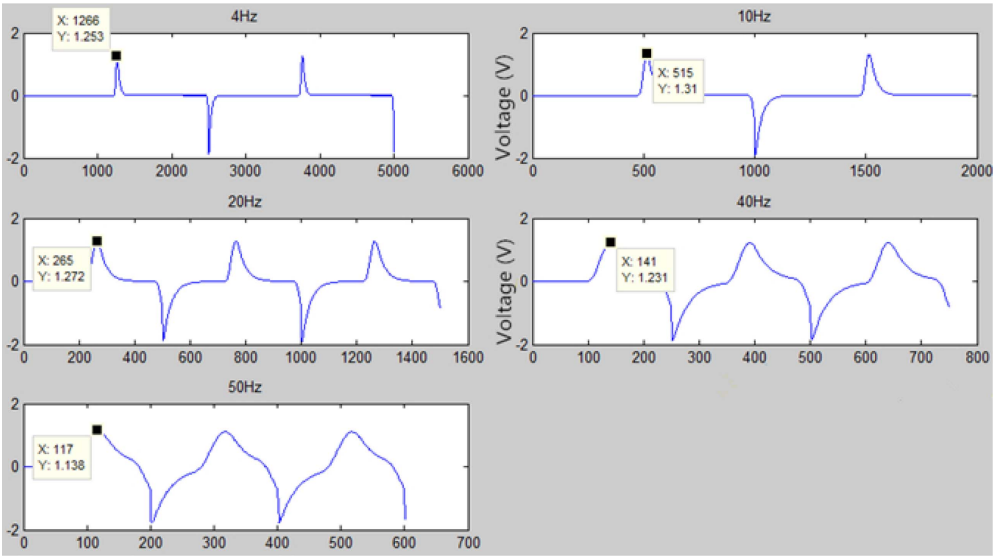

Fig. 6. (Color online) The effect of different excitation frequencies on the detection results.

increases with the number of turns, while the current in the coil will decrease. If the inductance is too large, the jump signal of the square wave excitation signal will be no longer steep along the abrupt change signal, but tend to be smooth, resulting in a distortion. The advantage of pulse excitation is that the steep jump of square wave keeps along the contained multi frequency signal. If it tends to smooth, it will lose its own advantages, which may seriously affect the reliability of the detection results.

Figure 7 shows the square wave exciting signal with frequency of 10 Hz and current of 5 V. When the turns of the excitation coil are selected with 170 turns, 180 turns, 200 turns, 250 turns and 300 turns, the shape of square wave current in the excitation coil is shown in Fig. 8. As the number of turns increases, the current decreases and the jump of the square wave current signal increases along the deformation. By comparing the simulation results, the

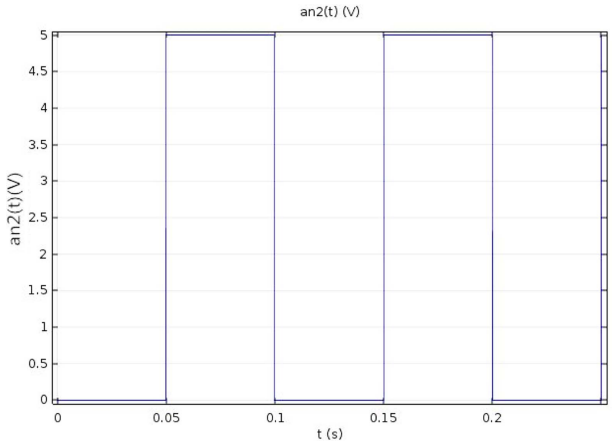

Fig. 7. (Color online) Square wave excitation signal.

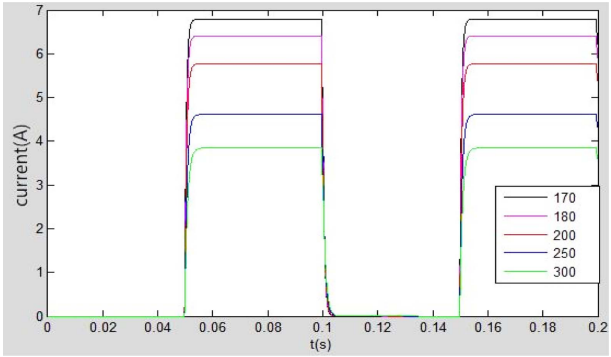

Fig. 8. (Color online) Current in the excitation coil with different turns.

number of turns of the excitation coil is selected to be 170 turns.

3.2.2.2. Number of turns of detection coil

Formula 25 shows the induction electromotive force of detection coil, where, N is the number of turns of coil, A is the cross sectional area of the coil, and θ is the angle between the axis of the coil and the direction of magnetic flow.

$$E = -N\frac{d\phi}{dt} = -NA\cos\theta\frac{dB}{dx}\frac{dx}{dt} \tag{32}$$

As known from formula 32, the induction electromotive force of the coil is proportional to the number of turns N and the cross sectional area A of the coil. The greater the number of turns of the coil and the cross sectional area of the coil, the greater the induction electromotive force will be. Therefore, the detection coil can get higher sensitivity.

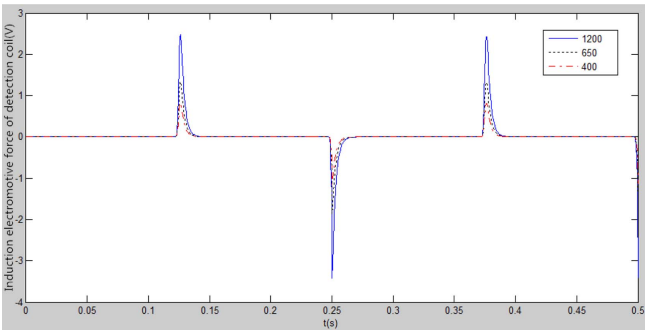

Fig. 9. (Color online) Influence of different turns of detection coil on induction electromotive force.

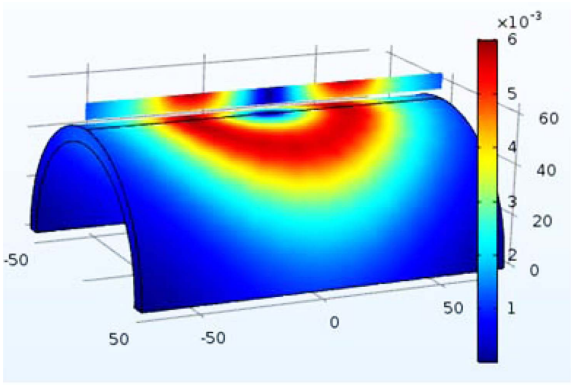

Fig. 11. (Color online) Induction current density mode.

Meanwhile, 10 Hz excitation frequency and 170 turns of excitation coil is selected, as the simulation results shown in Fig. 9. The more turns of the coil, the greater the induction voltage will be. Therefore, in order to improve the detection effect, the number of turns of the detection coil should be increased as much as possible. However, the number of turns of the detection coil is greatly limited by its size. It is necessary to select the proper number of coils at the same time as the design requirements are met. Hence the number of the detection coil is selected as 650 turns.

3.3. Analysis of simulation results

In the finite element model, the excitation coil adopts enameled copper wire with the diameter of 1 mm and the conductivity of 5.998e7s/m, a total of 170 turns; while the detection coil adopts enameled copper wire with the diameter of 0.2 mm and the conductivity of 5.998e7s/m, a total of 170 turns; the lift height of the coil is 1 mm, the square wave excitation voltage is 10 Hz and 5 V signal. Fig. 10 shows the flux density module and the section of the pipe wall at 0.28s time, while Fig. 11 shows the induction current density mode and mid-section view of pipe wall.

As seen from the magnetic flux density, the magnetic field intensity is larger in the covered area of the coil. From the cross-sectional view of magnetic flux density module, it can be directly observed that the strength of the magnetic field shows a decreasing trend as the magnetic lines increase the penetration depth in the pipe wall. The induced current density model shows the magnitude of the induced current density in the pipe wall. The induced current in the area beneath the excitation coil is larger. Because of the conductor skin effect, the induction current density decreases significantly as the depth increases. As shown in Figs. 10 and 11, the selected excitation meets the requirements of the pipeline depth detection.

On the rising edge and the falling edge of the square wave signal, the signal received by the detection coil is voltage signal that decays exponentially after a large increase. The transient magnetic field produced by pulse excitation generates vortex in the pipe wall. The reflected magnetic field produced by exponential decay of the eddy current is received by detection coil. The patterns of manifestation of the ultimate detection signal of finite element method is the voltage signal shown in Fig. 12. It can be seen that results gained by the theoretical model are consistent with those gained by finite element model.

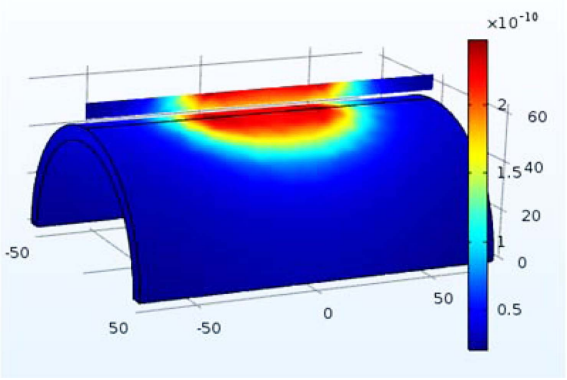

Fig. 10. (Color online) The flux density model in the model.

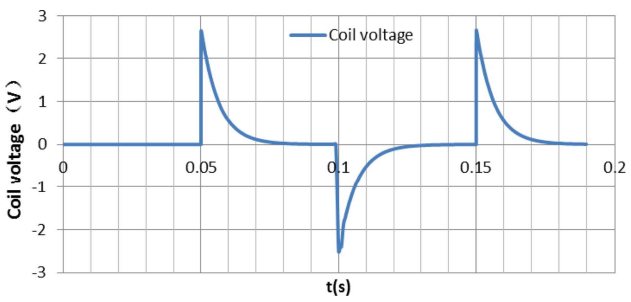

Fig. 12. (Color online) 10 Hz excitation detecting voltage signal.

There is a pulse width Δ between the first rising edge and the first falling edge. And a pulse period happens between the first rising edge and the second rising edge, which refers to *T*.

4. Experiments

4.1. Experimental system of PEC detection

PEC testing system mainly includes signal generator, excitation power supply, square wave conditioning circuit, sensor coil, and signal processing circuit, oscilloscope and signal acquisition, as shown in Fig. 13.

With the signal source of the excitation signal, the signal generator provides adjustable frequency and duty ratio pulse square wave signals and sufficient power for sensor coil at the same time. The signal processing circuit amplifies and filters the detected signals to obtain stable and reliable detection signals.

4.2. Experimental environment and data

The PEC test system is as shown in Fig. 14.

The experiment designs pipe wall at thicknesses of 6 mm, 5 mm, 4 mm and 3 mm respectively. The excitation signal is square wave whose amplitude is 5 V, frequency is 10 Hz and duty ratio is 50 %.

4.3. Experimental data and analysis

It can be seen from the formula 17 that the received signal of eddy current testing is an exponential attenuation pulse signal. The 6 mm-thickness steel plate is taken as test sample. The peak signal detected by the actual amplified wave filtering is shown in Fig. 15.

Figure 16a and 16b respectively show the phases of induced voltage gained experimentally and calculated under the 4 conditions of air, water, gas, and solids mixture in oil pipe with thickness of 6, 5, 4 and 3 mm. The solid line is the experimental result, and the dotted line is the theoretical calculation result.

From Fig. 16a, after the induction voltage is transformed by Hilbert to calculate phase [20, 21], the experimental curves are in good agreement with the calculated curves. The error of the calculated value is very small relative to

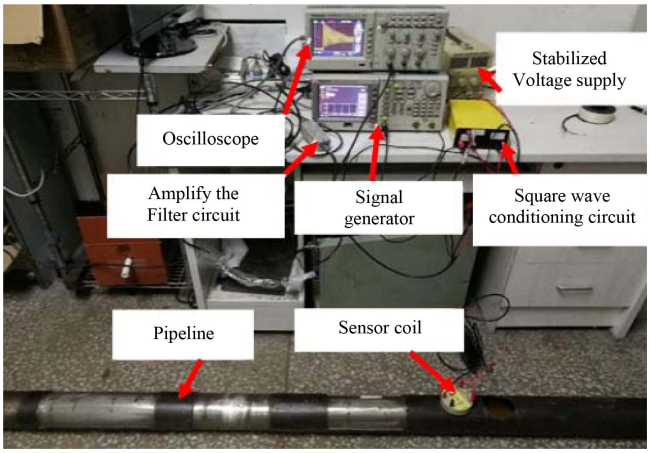

Fig. 14. (Color online) PEC detection system.

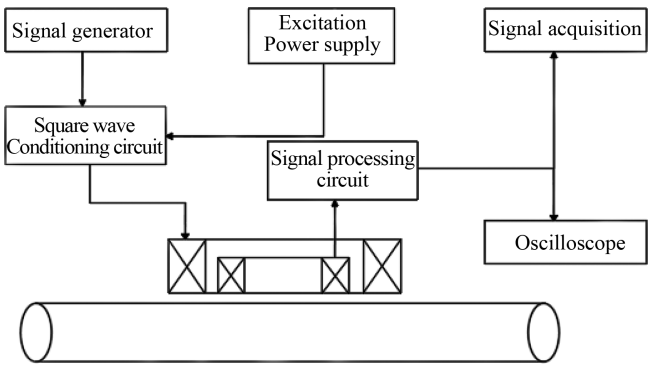

Fig. 13. Block diagram of PEC detection system.

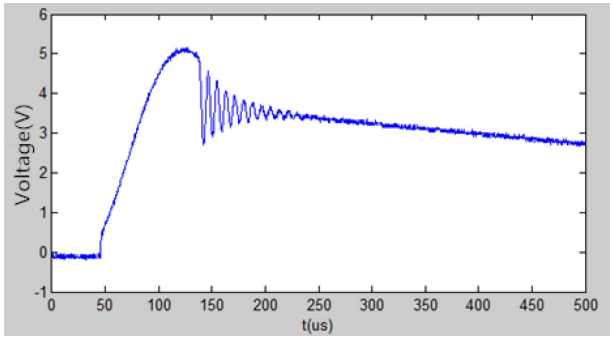

Fig. 15. (Color online) Peak signal after wave filtering.

Table 1. Relative detection parameters of sensor system.

Correlation parameters	Values	Correlation parameters	Values
Relative permeability of 20 steel	250	Outer diameter of excitation coil mm	80
Inside diameter of excitation coil mm	50	Inner diameter of detection coil mm	20
Lift height mm	1	Outside diameter of detection coil mm	34
Number of turns of excitation coil	170	Turns of detection coil	650
Excitation coil height mm	15	Detection coil height mm	10

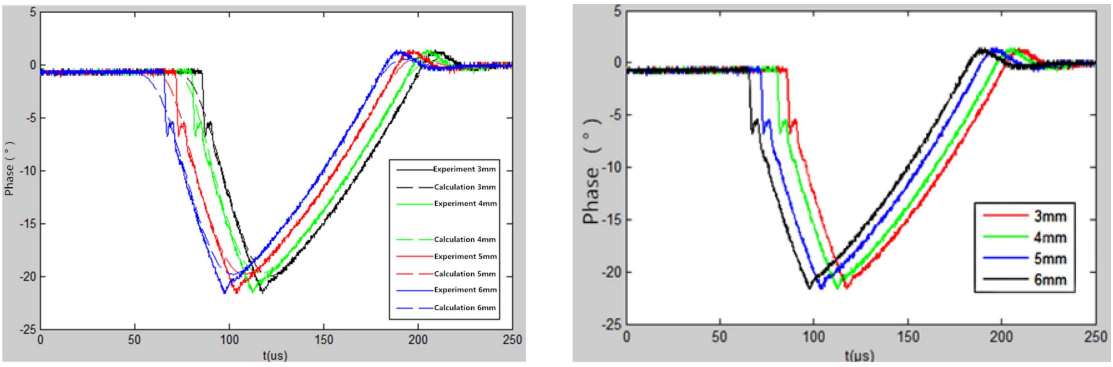

(a) Experimental curve and calculation curve of induction voltage phase for air

(b) Experimental phase curve of induction voltage for air, water, gas and solid mixture

Fig. 16. (Color online) Experimental curves of induction voltage phase in different media.

the experimental value within the noise margin. At the same time, different transmission media have little influence on the phase of induction voltage.

Trough time-wall thickness curve is shown in Fig. 17. Trough time varies linearly with wall thickness. The coefficient of linear fit is greater than 0.9966. The linear equations corresponding to the air medium and the mixed medium are:

$$y = -6.8000x + 138.6000,\ y = -6.9800x + 139.3100 \tag{32}$$

The characteristics of phase detection signal wave in time domain is below:

As the thickness of the tube decreases, the phase of the trough is delayed to the right in the time domain. As shown in Table 2 and 3, the phase delay is 6-8 us for each thinned 1 mm, which is independent of the media inside the pipe. A linear law exists, as shown in Fig. 17.

Table 2. Phase trough time for air.

Tube thickness/mm	Phase time/us
3	118
4	112
5	104
6	98

Table 3. Phase trough time for air, water, gas and solid mixture.

Tube thickness/mm	Phase time/us
3	117.8
4	112.5
5	103.9
6	97.4

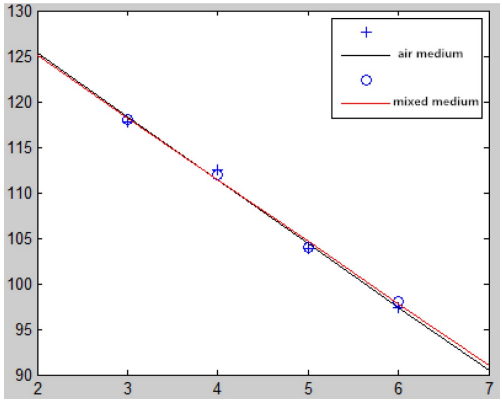

Fig. 17. (Color online) Changes (markers) and linear fitting (solid lines) of trough time varying with wall thickness under different media.

5. Conclusions

In conclusion, the PEC test with coaxial double coil structure can detect the pipeline residual wall thickness in the oil and gas gathering station. The expressions of induction voltage phase of magnetic induction coil of ferromagnetic tubing under PEC excitation are obtained. The finite element software COMSOL is used to study the finite element model of residual wall thickness of process pipe, which optimizes coil parameters and the excitation signal parameters, and designs PEC testing system. Meanwhile, the practicability of this method in detecting process pipe residual thickness is verified by experiments. Then, a method for evaluating the residual wall thickness of pipelines based on the phase trough time of induction voltage is proposed. The effectiveness of the proposed method is verified by the signals measured from PEC test of residual wall thickness in process pipeline.

The result shows that this method can meet the requirement of actual test. Additionally, the resolution and reliability of PEC testing are better in case of thinning 1-3 mm in the pipe with a thickness of 6 mm through experimental analysis. When different fluids pass through the pipeline, it can also achieve good detection results.

Acknowledgments

The authors acknowledge the National Natural Science Foundation of China (Grant: 21204139), the open Fund of Key Laboratory of Oil & Gas Equipment, Ministry of Education (Southwest Petroleum University) (Grant: OGE 201701-03).

References

[1] W. Zheng, China Pet. Chem. Stand. Qual. **5**, 254 (2013).
[2] S. X. Wang, Oil-Gas field Surf Eng. **22**, 70 (2003).
[3] J. Deng, Z. W. Xu, and C. X. Yi, Aviat Maint & Eng. **3**, 62 (2004).
[4] H. Zhang, B. F. Yang, Y. F. Jing, J. L. Li, and W. Y. Cui, Chinese J. Sens and Actuat. **25**, 1370 (2012).
[5] J. M. Lin, Nondestruct Test. **34**, 1 (2012).
[6] S. M. Haugland, IEEE Trans. Magn. **34**, 3195 (1996).
[7] A. Sophian, G. Tian, and M. Fan, Chin. J. Mech.-En. **30**, 500 (2017).
[8] D. Q. Zhou, B. Q. Zhang, and G. Y. Tian, Chinese J. Sci. Instrum. **30**, 1190 (2009).
[9] C. Y. Xiao and J. Zhang, Chinese Phys. B **19**, 120302 (2010).
[10] I. Z. Abidin, G. Y. Tian, J. Wilson, S. Yang, and D. Almond, NDT. & E. Int. **43**, 537 (2010).
[11] Y. He, G. Y. Tian, M. Pan, D. Chen, and H. Zhang, Corros Sci. **78**, 1 (2014).
[12] X. J. Wu, Q. Zhang, and G. T. Shen, Chinese J. Sci. Instrum. **37**, 1698 (2016).
[13] X. Chen and Y. Lei, Ndt & E Int. **73**, 33 (2015).
[14] D. Q. Zhou, G. Y. Tian, H. T. Wang, and L. H. You, Nondestruct Test. **10**, 25 (2011).
[15] H. Zhang, B. F. Yang, X. F. Wang, and Y. F. Zhao, J. Af. Eng. Univ. **13**, 52 (2012).
[16] X. L. Chen and Y. Z. Lei, Acta Phys. Sin.-Ch. Ed. **63**, 20 (2014).
[17] Z. J. Zhou, H. Wang, S. F. Zheng, and W. Zhou Wei, Electronics Quality. **9**, 18 (2009).
[18] T. Tian and K. Ding, Journal of Vibration and Shock. **2**, 23 (1996).
[19] Z. Z. He, F. L. Luo, B. Liu, and B. F. Yang, Journal Papers **31**, 810 (2009).
[20] Z. J. Zhou, H. Wang, S. F. Zheng, and W. Zhou, Electron Qual. **9**, 18 (2009).
[21] Q. S. Cheng, Petrol Geophys Prospect. **14**, 1 (1979).